Journal of Power Sources 223 (2013) 306–311

Contents lists available at SciVerse ScienceDirect

Journal of Power Sources

journal homepage: www.elsevier.com/locate/jpowsour

A high-performance hard carbon for Li-ion batteries and supercapacitors application

Jiangfeng Ni [a,*], Youyuan Huang [b], Lijun Gao [a,*]

[a] School of Energy, Soochow University, Suzhou 215006, China
[b] BTR New Energy Materials Inc., Shenzhen 518000, China

HIGHLIGHTS

- A hard carbon (HC) material is introduced for energy storage application.
- The HC delivers a high capacity of 526 mAh g^{-1} with coulombic efficiency of 80%.
- The constructed $Li(Ni_{1/3}Co_{1/3}Mn_{1/3})O_2$/HC battery shows superior rate capability.
- The activated carbon/HC hybrid capacitor exhibits a high level of energy and power.

ARTICLE INFO

Article history:
Received 10 May 2012
Received in revised form
8 August 2012
Accepted 14 September 2012
Available online 3 October 2012

Keywords:
Hard carbon
Lithium ion battery
Supercapacitor
Electrochemical performance
Power capability

ABSTRACT

A hard carbon (HC) prepared from phenolic resins is investigated as a potential electrode material for power Li-ion batteries and hybrid supercapacitors. The electrochemical test results indicate that the HC is capable of delivering a capacity of 526 mAh g^{-1} (about 40% greater than graphite) with an initial coulombic efficiency of 80%. The constructed $Li(Ni_{1/3}Co_{1/3}Mn_{1/3})O_2$/HC full cells shows superior power capabilities, retaining 90% of reversible capacity at a discharge rate as high as 30 C. That is equivalent to a specific energy of 98 Wh kg^{-1} at a power of 3000 W kg^{-1}. When combined with an activated carbon (AC), the constructed AC/HC hybrid capacitor exhibits a specific capacitance of 21.5 F g^{-1} or energy density of 22.6 Wh kg^{-1} (considering the weight of all components of the full cell) at a current of 100 mA g^{-1}. At a power of 480 W kg^{-1}, it delivers an energy density of 20.8 Wh kg^{-1}, which is twice that of a conventional AC/AC supercapacitor. The feature of high energy and power capabilities makes HC materials promising candidates as electrodes for energy storage and conversion application.

1. Introduction

Hard carbon (HC) is one of the promising carbonaceous materials for energy storage and conversion application, including Li-ion batteries and supercapacitors. Generally, HC is a kind of carbon that is difficult to be graphitized, and usually it is prepared from pyrolysis of polymers such as phenolic resin, epoxy resin [1–3]. From the structural viewpoint, HC is highly irregular and disordered, and it is primarily consisted of single-layer carbon atoms that are closely and randomly connected. Such a stack fashion contrasts with graphite in which carbon atoms form hexagons in the same plane, and the planes are connected by Van der Waals' force. Thus, a "falling card" model was proposed to describe the structure of HC [4]. Since lithium ions can intercalate and be adsorbed in both sides of carbon graphene sheet, a higher theoretical capacity twice that of graphite material can be reached up to 500–700 mAh g^{-1}. Moreover, the space gap between the adjacent carbon layers is larger than graphite materials, which is beneficial for Li ion mobility. As a result, HC displays a high level of energy and power, which is particularly desirable for power sources used in automobiles and power tools.

Recently, many works involving the application of HC materials as anodes for Li-ion batteries have been reported. The HC electrodes have demonstrated favorable characteristics compared with the graphite anode, including higher capacity, longer life, better rate performance, and improved safety [5–11]. Specifically, Haruna et al. demonstrated that lithium manganese oxide/HC batteries could meet the targets of energy density and lifespan for automobile application [9]. However, HC materials also exhibit some drawbacks, including large irreversible capacity, low pack density, and

* Corresponding authors. Tel./fax: +86 512 65229905.
E-mail addresses: jeffni@suda.edu.cn (J. Ni), gaolijun@suda.edu.cn (L. Gao).

0378-7753/$ – see front matter © 2012 Elsevier B.V. All rights reserved.
http://dx.doi.org/10.1016/j.jpowsour.2012.09.047

hysteresis in the voltage profile. It is believed that such drawbacks are intimately related to the physical and chemical characteristics of HC like stacking fashion, pore size and distribution and impurities. Therefore, modifications to address these issues such as coating with carbon [7], introducing a secondary phase [6,8], or oxidizing treatment [10] could manipulate the capacity delivery and efficiency. Alternatively, Liu et al. proposed a battery configuration composed of $xLi_2MnO_3\cdot(1-x)LiMn_{0.4}Ni_{0.4}Co_{0.2}O_2$ and HC to tackle the low coulombic efficiency issue [11]. In such a battery system, the irreversible capacity that occurs for both materials can be matched and well counter-balanced. Besides the potential application in Li-ion batteries, HC is also a suitable candidate electrode for sodium ion based batteries [12].

The feature of rapid kinetics of HC makes it also viable for application in supercapacitors. As novel energy storage system, supercapacitors receive great attention because of higher energy compared to conventional capacitors, while higher power and longer cycle life than batteries [13,14]. However, its energy density is limited in comparison with a battery, typically in the range of 5–7 Wh kg^{-1} [13]. To increase the energy density, asymmetric hybrid supercapacitors, involving an AC and a battery type electrode material, have been investigated intensively [15,16]. When combining an HC negative electrode with an AC positive one, the AC/HC constitutes an internal capacitor and battery hybrid system, which may improve the energy level while maintain power robustness and cycle performance simultaneously [17–19].

Previously, we have reported the property of an HC sample and its application in $LiFePO_4$/HC batteries [20]. The battery can be cycled at a charge and discharge rate of 10 C without appreciable capacity fading up to 2450 cycles. However, the low capacity (322 mAh g^{-1}) makes it not competitive with graphite and MCMB materials [8,11], thereby restricting the application. In this work, we report our progress in developing new-generation HC materials. The electrochemical property of the HC was evaluated in detail on $Li(Ni_{1/3}Co_{1/3}Mn_{1/3})O_2$/HC full batteries and AC/HC hybrid supercapacitors. The results demonstrate that the HC material shows promising features in terms of energy density, power robustness, and cycle stability.

2. Experimental

The HC sample was prepared by pyrolysis of phenolic resin in argon atmosphere and at temperature about 1100 °C (BTR New Energy Materials Inc.). The HC material was used as received without further treatment.

For battery test, HC negative electrodes were prepared from a slurry containing 93 wt.% hard carbon, 2 wt.% conductive carbon (Super-P-Li, Timcal), 2.5 wt.% thickening agent carboxymethyl cellulose sodium (CMC), and 2.5 wt.% of binder styrene butadiene rubber (SBR). The slurry was casted by a doctor-blade process onto a 12-μm thick copper foil current collector. $Li(Ni_{1/3}Co_{1/3}Mn_{1/3})O_2$ positive electrodes were prepared by homogeneously mixing 90 wt.% active material, 5 wt.% Super-P-Li, and 5 wt.% polyvinylidene difluoride (PVDF) dispersed in N-methyl-2-pyrolidone (NMP). The formed slurry was coated on an aluminum foil of 20-μm thickness. After drying at 100 °C in a vacuum for 12 h, both HC and $Li(Ni_{1/3}Co_{1/3}Mn_{1/3})O_2$ electrodes were roll pressed and slit. The electrodes were wound with separators into a prismatic assembly and placed into a cell can with dimensions of 6.0 × 30 × 48 mm^3. The electrolytic solution is 1.3 mol l^{-1} $LiPF_6$ dissolved in EC/DMC (1:3 by volume).

For the hybrid capacitor test, the AC electrode was fabricated by laminating 85 wt.% AC (YP–17D, Kuraray, Japan), 5 wt.% Super-P-Li, 5 wt.% conductive graphite KS, and 5 wt.% PVDF slurry on an aluminum foil (20 μm). The electrode sheet was dried at 100 °C for 12 h and roll pressed to a certain thickness. Disks with diameter of 12 mm were pouched out of the laminate to make positive electrodes. HC electrode disks with the same size were used as negative electrodes. The AC/HC hybrid capacitors were assembled in a glove box (MBraun) filled with argon atmosphere using Celgard 2325 as separator and 1 mol l^{-1} $LiPF_6$ in EC/DMC (1:3 by volume) as electrolyte.

The half cell performance of HC electrode was also evaluated separately using lithium metal as the counter electrode. The charge and discharge tests were performed on a LAND battery test system (Jinnuo, China) controlled by a computer at room temperature. Electrochemical impedance spectra (EIS) were recorded on an IM6e electrochemical workstation (Zahner, Germany).

Crystallographic structure of the HC was identified by X-ray diffraction (XRD) on a D/Max-IIIA diffractometer (Rigaku, Japan) using Cu kα ($\lambda = 0.15406$ nm) as radiation source. The morphology of the samples was observed using scanning electron microscopy (SEM, Hitachi-4800, Japan) and transmission electron microscopy (TEM, JEOL JEM-2010, Japan). The specific surface area and pore distribution was measured on an automated area and pore size analyzer (Quadrasorb SI, Quantachrome Instruments, USA). The size distribution was measured using a laser particle analyzer (Mastersizer 2000, Malvern, UK).

3. Results and discussion

3.1. Physicochemical characterization

Table 1 shows some physicochemical parameters of the HC sample. The HC material exhibits a mean particle size of 12.8 μm and a surface area of 11.6 m^2 g^{-1}. This surface area is much higher that of the previous HC material (1.2 m^2 g^{-1}) reported in ref. [20], due to a unique porous structure of the new HC material. The average interlayer space is calculated to be 0.431 nm using method of Azuma et al. [2], larger than that of graphite.

X-ray diffraction pattern of the HC carbon composites is shown in Fig. 1. The peaks at 24.8°, 43.6°, and 79.5° are correlated to (002), (100), and (110) diffraction peaks. The crystallite sizes of Lc and La determined from the (002) and (100) diffraction peaks are 1.50 and 1.76 nm, respectively, using the Scherrer equation. Liu et al. defined an empirical parameter *R* that refers to the ratio of the height of the (002) peak against the background, to estimate the fraction of single-layers in hard carbon materials [3]. In general, the larger the *R* is, the less the fraction of single layers is. In this case, the large *R* of 3.2 suggests that the content of single layer is not high.

Fig. 2a and b show the SEM images of the cross-section of HC particles. It can be observed that HC particles exhibit a size of ~10 μm, with many mesopores dispersed inside. A close examination shows that the pore size is in the range of 20–50 nm, which is quite different from the mean pore size of 1.92 nm obtained by the N_2 adsorption experiments, as shown in Fig. 2d. This discrepancy is possibly because that most micropores may not be observed by SEM imaging due to limitation of magnitude. Fig. 2c shows a TEM image of the HC, in which the local layer structure can be clearly observed. However, the ordering of carbon layer in HC is limited to a few layers, which is in contrast to perfect arrangement of carbon layers in graphite. Although single layered graphenes are

Table 1
Physicochemical characteristics of the hard carbon material.

D_{10} (μm)	D_{50} (μm)	D_{90} (μm)	BET (m^2 g^{-1})	Pore size (nm)	Porosity (%)	True density (g cm^{-3})
3.0	12.8	33.6	11.6	1.92	22.1	1.76

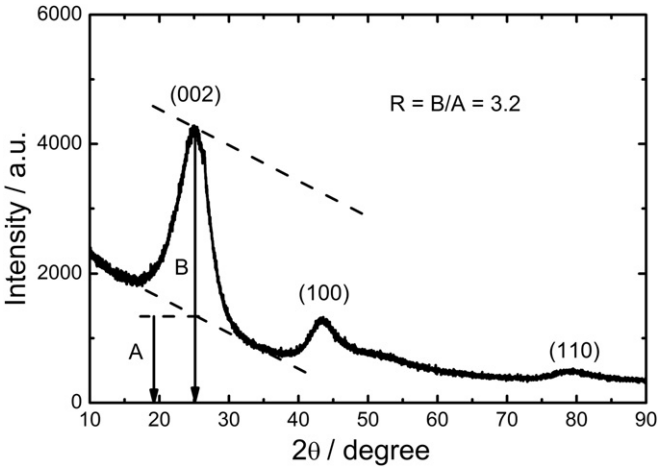

Fig. 1. XRD pattern of the hard carbon material.

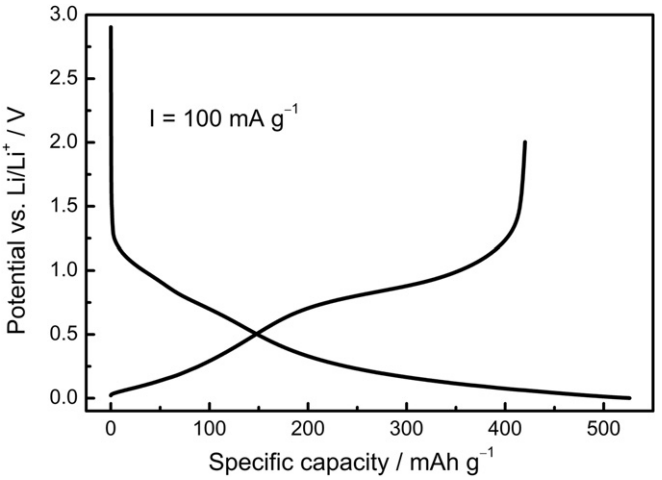

Fig. 3. Initial charge/discharge profile of HC/Li half cell at 100 mA g^{-1} between 0 V–2.0 V vs. Li/Li$^+$.

difficult to be identified, the presence of graphene bilayer and trilayer are clearly visible in an abundant amount, as marked by arrows in Fig. 2c.

3.2. Evaluation in Li cells

Previously, a HC material was reported showing a capacity of 322 mAh g^{-1} with an initial coulombic efficiency of 83% [20]. Although the rate capability and cycle life results were impressive, the capacity was low and thus not competitive with the graphite anode. The newly developed HC sample in this work shows a significant improvement in Li storage capacity, as it is revealed by the half cell performance shown in Fig. 3. In the potential range of 0–2.0 V vs. Li/Li$^+$, a capacity of 526 mAh g^{-1} with an efficiency of 80% can be achieved when coupled with a lithium metal anode, about 63% greater than that of the previous HC. This capacity is not only superior to those of many others reported HC materials [7,8,11], but also 40% greater than that of graphites (372 mAh g^{-1}). It is believed that a more disordered structure and abundant pores (porosity 22.1%, Table 1) may account for the enhanced performance.

To probe the charge and discharge behavior in depth, the incremental capacity vs. potential (dQ/dV) is plotted in Fig. 4. It can be seen that a subtle cathodic peak emerges at 0.99 V vs. Li/Li$^+$ during the first Li intercalation process, which is due to the formation of surface protection layer (known as SEI). The redox pairs at 0.78/0.83 V may be due to the insertion/extraction of lithium between carbon layers where they are stacked in a more parallel model (multi-layered graphene), whereas those near 0 V are due to the Li adsorption/desorption in both sides of single sheets or walls of nanopores [3]. For clarification, the inset in Fig. 4 shows the possible Li storage mechanism in HC material. It is clearly

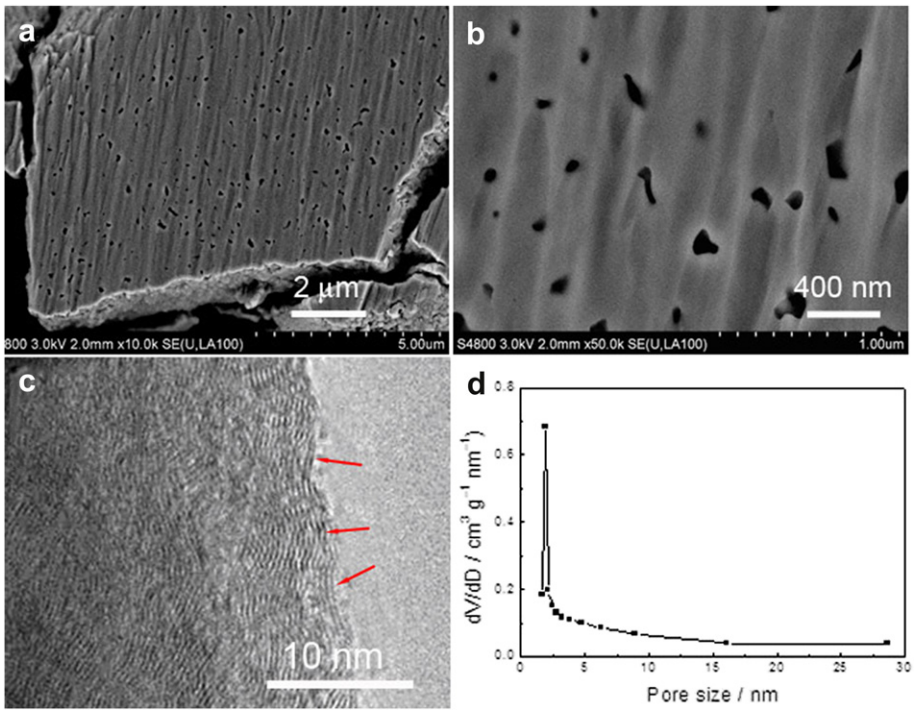

Fig. 2. (a and b) SEM, (c) TEM images, and (d) pore size distribution of the hard carbon material. Arrows in (c) mark graphene bilayers or trilayers.

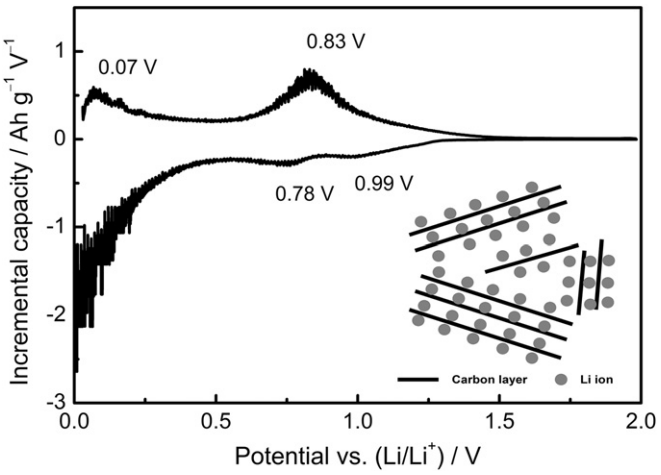

Fig. 4. Incremental capacity of the HC/Li half cell derived from Fig. 3. Inset shows the possible Li storage mechanism in hard carbon [3].

seen that one carbon layer can store more than one layer of Li ions, resulting in a capacity beyond that of LiC_6 (372 mAh g^{-1}). Redox peaks near 0.25 V due to side reactions of lithium with surface functional groups or absorbed species are absent, implying the material is not sensitive to atmosphere [6]. In addition, the capacity delivery of HC occurs in a wide potential range as shown in discharge curve in Fig. 3, quite different from graphitic carbon. As a result, the formation of Li dendrite in HC anode could, to a large extent, be suppressed.

The Li storage property of the HC materials was further evaluated by $Li(Ni_{1/3}Co_{1/3}Mn_{1/3})O_2$/HC full batteries. Fig. 5a presents the discharge profiles of an optimal $Li(Ni_{1/3}Co_{1/3}Mn_{1/3})O_2$/HC battery at various rates. The battery is charged at a constant current–constant voltage (CC–CV) protocol of 1 C rate to 4.2 V and then discharged to 2.0 V. At a 1 C rate, the battery discharges a capacity of 847 mAh. When the discharge rate increases to 10 C, the battery can hold up 91% of capacity. Further increasing the rate to 30 C results in negligible capacity fading except for voltage drop, mainly due to Ohmic resistance. This rate capability is superior to those of many HC-based batteries found in references [9,10], which may be directly related to the unique porous structure [17]. To help understand the impressive performance, the $Li(Ni_{1/3}Co_{1/3}Mn_{1/3})O_2$/HC batteries using the previous HC material as anode is investigated and the result is compared in Fig. 5b. The battery only delivers a capacity of 737 mAh at 1 C, which is 13% less than that of a battery applying the newly-developed HC material. The capacity decreases to 668 mAh when the rate was raised to 10 C, and remains unchanged upon higher current rates. However, the discharge profiles upon high rates exhibit large voltage drops and almost lose the original shape, indicating a severe electrochemical polarization due to poor kinetics. The discrepancy in the performances is explainable in terms of the differences in the structural characteristic. The new HC material consists of a large amount of pores and voids whereas the previous one is less porous. These pores can adsorb extra Li ions and thus enhance the Li storage capacity. In addition, the porous structure can reduce the actual current density passing the electrode/electrolyte interphase by increasing the reaction area, leading to a better rate discharge capability.

Fig. 6 displays the Ragone plot of the $Li(Ni_{1/3}Co_{1/3}Mn_{1/3})O_2$/HC full battery to show the dependence of specific energy (SE) on specific power (SP). The SE is calculated based on the whole energy delivery and the mass of the entire battery (~22 g), whereas the SP refers to the power at 50% depth of discharge. As can be seen, the SE decreases gradually as the power output increases. At a low power

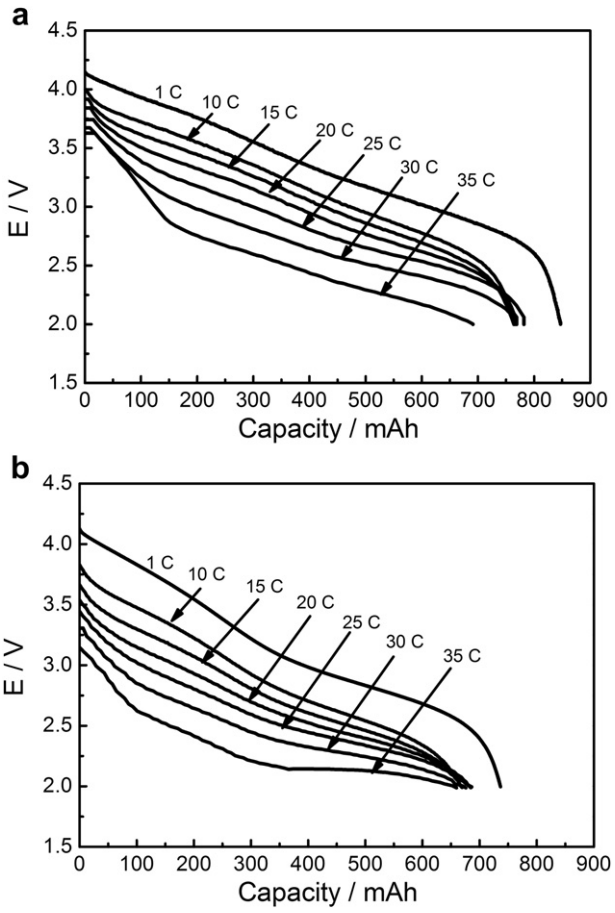

Fig. 5. Rate discharge capability of the $Li(Ni_{1/3}Co_{1/3}Mn_{1/3})O_2$/HC Li-ion batteries applying (a) the new HC anode and (b) the previous HC anode.

of 130 W kg^{-1}, the SP is 130 Wh kg^{-1}. When the power increases to 3000 W kg^{-1} (30 °C), the energy density still reaches 98 Wh kg^{-1}. This result is comparable in power but higher in energy than a battery adopting $Li_5Ti_4O_{12}$ nanomaterial, due to lower Li intercalation potential of HC electrode [21]. For comparison, Fig. 6 also shows the performance of $Li(Ni_{1/3}Co_{1/3}Mn_{1/3})O_2$/graphite batteries assembled at the identical condition. In the whole range of power, the SE of graphite-based battery is below that of HC-based one. Increasing the power from 130 W kg^{-1} to 800 W kg^{-1} leads to a dramatic drop in energy from 115 Wh kg^{-1} to 64 Wh kg^{-1}. When

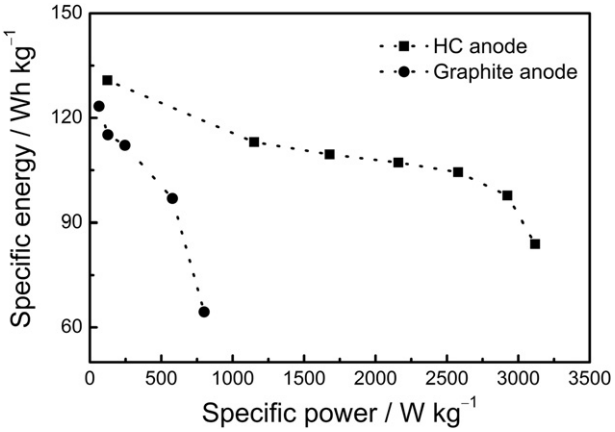

Fig. 6. Ragone plots of the $Li(Ni_{1/3}Co_{1/3}Mn_{1/3})O_2$/HC and $Li(Ni_{1/3}Co_{1/3}Mn_{1/3})O_2$/graphite batteries.

applied power goes beyond 1200 W kg^{-1}, the battery can hardly be discharged.

3.3. Evaluation in AC/HC hybrid supercapacitors

To investigate the capacitive behavior of HC, prototype supercapacitors were constructed and examined by using AC positive and HC negative electrodes containing 1 mol l^{-1} $LiPF_6$ in EC/DMC electrolyte. The mass of the electrodes was balanced to fully take profit of the performance of both materials in their optimal working potential range. The rate capability of such a mass-balanced AC/HC hybrid cell was examined at various discharge rates as shown in Fig. 7a. The charge and discharge profile of a conventional symmetric AC/AC capacitor is also shown in Fig. 7b. With the increase of current rate, the discharge time reduces while the profile almost remains the same in the voltage range of 4.0–2.8 V (Fig. 7a). The cell voltage profile declines with time as a capacitor should be, however the slope is not strictly linear. This result indicates that the hybrid supercapacitor exhibited discharge characteristics of the combination of a capacitor and a battery [22].

The specific capacitance of C_m of such an AC/HC hybrid supercapacitor at various currents can be calculated by the following formula:

$$C_m = \frac{i \times \Delta t}{m \times \Delta V} \quad (1)$$

where i (A) represents the discharge current, ΔV (V) the discharge voltage variation (exclude the IR drop), Δt (s) the discharge time consumed in the voltage change range of ΔV. The mass used in calculation involves the entire hybrid supercapacitor (including both electrode materials, current collectors, electrolyte and separator). With the increase of discharge current from 100 mA g^{-1} to 400 mA g^{-1}, the specific capacitance of the hybrid supercapacitor only changes from 21.5 to 20.7 F g^{-1}. In contrast, the capacitance of the AC/AC capacitor is calculated to be 12.0 F g^{-1} at 200 mA g^{-1}, which is only 56% of that of the hybrid AC/HC system. These results suggest that the hybrid capacitors are capable of delivering a higher capacitance with favorable rate capability. Since the AC material is known to be high rate capable based on its principle of ion diffusion in double layer, and the HC has numerous micropores and expanded carbon inter-plane space that provide active sites for fast Li insertion/extraction surface reaction, thus the high charge-storage capability and robust rate performance of AC/HC hybrid cells could be realized [23].

The specific energy was calculated from $E = 1/2C_m(V_2 - V_1)$, where $V_2 = 4.0$ V and $V_1 = 2.8$ V [22]. The specific power was obtain from $P = I\,\Delta V/m = i\,(V_2 - V_1)$, where i is the current density in mA g^{-1}. The results demonstrates that the specific energy is 22.6 Wh kg^{-1} at a power of 120 W kg^{-1}; when the power reaches 480 W kg^{-1}, the energy remains at 20.8 Wh kg^{-1} for the AC/HC hybrid supercapacitor. This energy density is about twice that of the conventional AC/AC system, which is calculated to be 10.4 W kg^{-1}. Therefore, this AC/HC hybrid supercapacitor presents an alternative approach to meeting the requirements of EV power sources.

Fig. 8 shows the cycle life results of the AC/HC hybrid supercapacitor at a charge–discharge current of 200 mA g^{-1}. The hybrid cell displayed a stable behavior over a long cycle time at such a high cycle rate. After 3000 cycles the specific capacitance retains 90.4% of the initial value. It is also seen that the coulombic efficiency increases gradually upon initial cycles, allowing some time for the system to be stabilized, then maintains at a level close to 100%.

To further understand the electrochemical process of the AC/HC hybrid supercapacitor, EIS experiments were carried out on the AC/HC supercapacitor and compared with an AC/AC one. Fig. 9 illustrates the Nyquist plots of the impedance spectra of the two supercapacitors. The spectrum of AC/HC supercapacitors consists of two depressed semicircle in high and middle frequency and a straight line in low frequency. The semicircle in the high frequency region is due to the surface layer (SEI) formed on the HC electrode; the semicircle in the middle frequency represents the charge-transfer resistance (R_{ct}); and the straight is associated with Li ion diffusion in electrodes. In contrast, AC/AC capacitor only shows one semicircle related to charge-transfer resistance. The R_{ct}

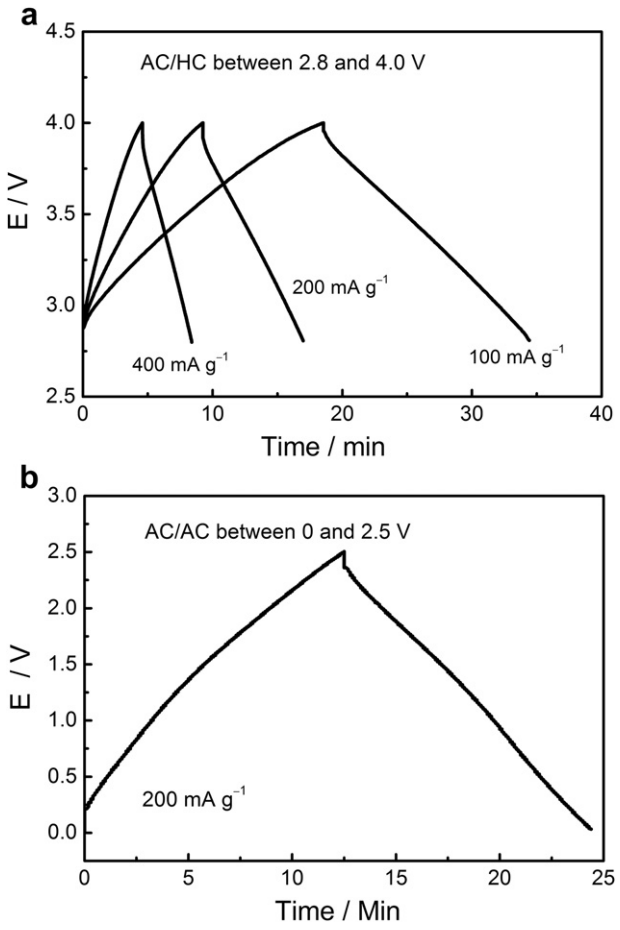

Fig. 7. Charge and discharge profiles of (a) the AC/HC hybrid supercapacitor at various rates and (b) the AC/AC capacitor at 200 mA g^{-1}.

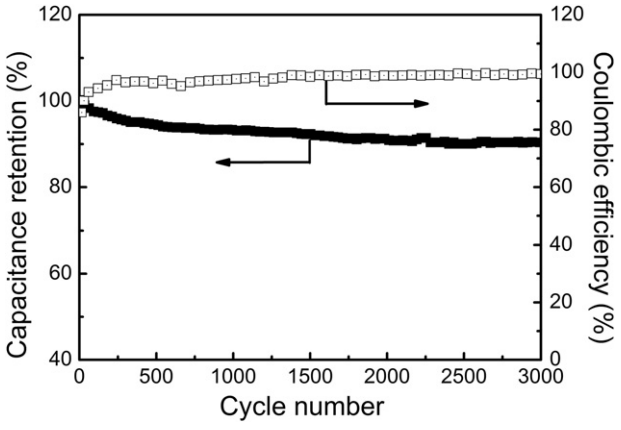

Fig. 8. Capacity retention and coulombic efficiency of the AC/HC hybrid supercapacitor cycled at a current of 200 mA g^{-1}.

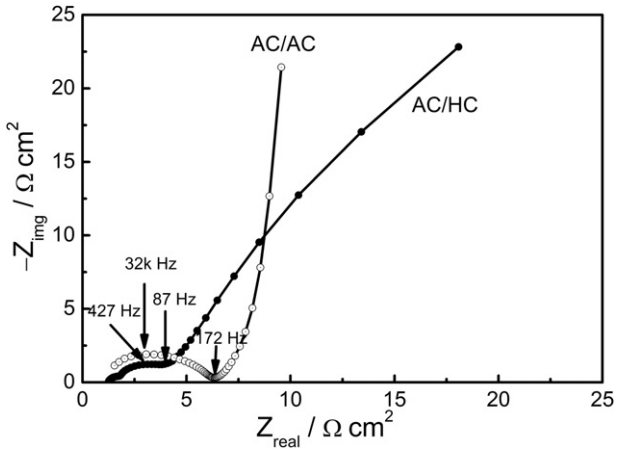

Fig. 9. Electrochemical impedance spectra of the AC/HC and AC/AC supercapacitors.

of AC/HC (1.6 Ω cm^2) is less than that of AC/AC (5.2 Ω cm^2), indicating that faster kinetics could be achieved in the former. Although the reason for the low R_{ct} has not been fully understood, it is possibly due to the surface layer on HC, as SEI is highly ionically conductive and may suppress side reactions between electrode and electrolyte. It is worth pointing out that the straight line of AC/HC spectrum deviates from vertical shape of the AC/AC capacitor, indicating that Li ion diffusion in the HC electrode is not a pure capacitive behavior [24].

4. Conclusion

In summary, a new generation hard carbon material derived from phenolic resin was prepared, and the feasibility of application in Li-ion batteries and hybrid supercapacitors was assessed. The electrochemical test results show that the HC electrode is capable of delivering a high capacity of 526 mAh g^{-1} with an initial coulombic efficiency of 80%. The intercalation of Li ion occurs mainly in the regions of 0 V and 0.8 V vs. Li/Li$^+$ with gradual change of potentials, manifesting Li adsorption/desorption at different sites in HC lattice. The constructed $Li(Ni_{1/3}Co_{1/3}Mn_{1/3})O_2$/HC battery shows a high energy level and excellent rate discharge capability. At a power of 3000 W kg^{-1}, it still delivers a specific energy of 98 Wh kg^{-1}. When coupled with AC positive electrodes, the AC/HC hybrid supercapacitor exhibits a specific energy of 20.8 Wh kg^{-1} at a power of 480 W kg^{-1}, which is twice that of an AC/AC system. After 3000 deep cycles at 200 mA g^{-1}, the hybrid cell retains 90% of initial capacitance. It is believed that the rapid kinetics is due to porous structure and expanded graphite sheet space. Investigation on long-term cycle stability of $Li(Ni_{1/3}Co_{1/3}Mn_{1/3})O_2$/HC batteries and optimization of AC/HC supercapacitors are in progress. The results will be summarized in our next study.

Acknowledgments

Financial support of National 863 Project (No. 2011AA11A235) is gratefully acknowledged.

References

[1] J.R. Dahn, T. Zheng, Y. Liu, J.S. Xue, Science 270 (1995) 590–593.
[2] H. Azuma, H. Imoto, S. Yamada, K. Sekai, J. Power Sources 81–82 (1999) 1–7.
[3] Y. Liu, J.S. Xue, T. Zheng, J.R. Dahn, Carbon 34 (1996) 193–200.
[4] J.R. Dahn, W. Xing, Y. Gao, Carbon 35 (1997) 825–830.
[5] J. Hu, H. Li, X. Huang, Solid State Ionics 178 (2007) 265–271.
[6] J.-H. Lee, H.-Y. Lee, S.-M. Oh, S.-J. Lee, K.-Y. Lee, S.-M. Lee, J. Power Sources 166 (2007) 250–254.
[7] H. Sun, X. He, J. Li, J. Ren, C. Jiang, C. Wan, Electrochim. Acta 52 (2007) 4312–4316.
[8] B. Guo, J. Shu, K. Tang, Y. Bai, Z. Wang, L. Chen, J. Power Sources 177 (2008) 205–210.
[9] H. Haruna, S. Itoh, T. Horiba, E. Seki, K. Kohno, J. Power Sources 196 (2011) 7002–7005.
[10] H. Fujimoto, K. Tokumitsu, A. Mabuchi, N. Chinnasamy, T. Kasuh, J. Power Sources 195 (2010) 7452–7456.
[11] J.-L. Liu, J. Wang, Y.-Y. Xia, Electrochim. Acta 56 (2011) 7392–7396.
[12] S. Komaba, W. Murata, T. Ishikawa, N. Yabuuchi, T. Ozeki, T. Nakayama, A. Ogata, K. Gotoh, K. Fujiwara, Adv. Funct. Mater. 21 (2011) 3859–3867.
[13] B.E. Conway, Electrochemical Supercapacitors: Scientific Fundamentals and Technological Applications, Kluwer Academic/Plenum Publishers, New York, 1999.
[14] B. Andrew, J. Power Sources 91 (2000) 37–50.
[15] Z. Chen, V. Augustyn, J. Wen, Y. Zhang, M. Shen, B. Dunn, Y. Lu, Adv. Mater. 23 (2011) 791–795.
[16] N. Yu, L. Gao, Electrochem. Commun. 11 (2009) 220–222.
[17] W. Xing, C.C. Huang, S.P. Zhuo, X. Yuan, G.Q. Wang, D. Hulicova-Jurcakova, Z.F. Yan, G.Q. Lu, Carbon 47 (2009) 1715–1722.
[18] J.-H. Kim, J.-S. Kim, Y.-G. Lim, J.-G. Lee, Y.-J. Kim, J. Power Sources 196 (2011) 10490–10495.
[19] Q. Li, R. Jiang, Y. Dou, Z. Wu, T. Huang, D. Feng, J. Yang, A. Yu, D. Zhao, Carbon 49 (2011) 1248–1257.
[20] X. Liao, J. Yu, L. Gao, J. Solid State Electrochem. 16 (2011) 423–428.
[21] K. Zaghib, M. Dontigny, A. Guerfi, P. Charest, I. Rodrigues, A. Mauger, C.M. Julien, J. Power Sources 196 (2011) 3949–3954.
[22] B.E. Conway, J. Electrochem. Soc. 138 (1991) 1539–1548.
[23] A.G. Pandolfo, A.F. Hollenkamp, J. Power Sources 157 (2006) 11–27.
[24] N. Yu, L. Gao, S. Zhao, Z. Wang, Electrochim. Acta 54 (2009) 3835–3841.